applied sciences

MDPI

Supplementary materials

Fluorescence Correlation Spectroscopy Combined with Multiphoton Laser Scanning Microscopy—A Practical Guideline

Jeemol James [1,*], Jonas Enger [2] and Marica B. Ericson [1,*]

[1] Biomedical photonics group, Department of Chemistry and Molecular Biology, University of Gothenburg, 41296 Gothenburg, Sweden
[2] Department of Physics, University of Gothenburg, 41296 Gothenburg, Sweden; jonas.enger@physics.gu.se
* Correspondence: jeemol.james@gu.se (J.J.); marica.ericson@gu.se (M.B.E.)

S1—Supplementary Theory

Theoretical Relation between the Diffusion Constant and Diffusion Time in the Context of Size of Detection

In two photon excitation (2PE), excitation volume is defined by point spread function [1,2]:

$$V = \pi^{3/2} w_{xy}^2 \omega_z \tag{1}$$

where w_{xy} and w_z are $\frac{1}{e^2}$ lateral and axial beam radius in XY and Z plane, respectively.

Diffusion constant (D) and translational diffusion time (τ_D) are related by:

$$\mathrm{D} = \frac{w_{xy}^2}{8\tau_D} \tag{2}$$

Ratio of translation diffusion time generated by 40X and 63X objective lenses are

$$\frac{\tau_D(40X)}{\tau_D(63X)} = \frac{w_{xy}^2(40X)}{w_{xy}^2(63X)} \tag{3}$$

From the theoretical calculation this ratio should be 2; however, based on the data included in manuscript (see Figure 3), the acquired ratio is larger by a factor of 300.

Theoretical Relation Between the Ratio of Area and Detection Volume with Normalized Excitation Power in The Context Of Fick's Law

Approximating the detection volume as a sphere, the surface area of a sphere is

$$A = 4\pi r^2 \tag{4}$$

where r is the radius of the detection volume. In analogue, the volume of the sphere

$$V = \frac{4}{3}\,\pi r^3 \tag{5}$$

Ratio of area to volume

$$\frac{A}{V} = 3\,\frac{1}{r} \tag{6}$$

In 2PE, the excitation power distribution at a point x follows a Gaussian function as

$$I_{(x)} = \frac{I_0}{\omega\sqrt{2\pi}} e^{-x^2/\omega^2} \tag{7}$$

Because of the square intensity dependency, this can be written as:

$$I^2_{(x)} = \frac{I_0^2}{\omega^2 2\pi} e^{-2x^2/\omega^2} \tag{8}$$

The threshold determining the excitation volume can be set for two different laser powers corresponding to two different cases such as:

Case 1: at low excitation power, threshold at x= ω_1]

$$I^2_{(\omega_1)} = \frac{I^2_{0,1}}{{\omega_1}^2 2\pi} e^{-2} \tag{9}$$

Case 2: at high excitation power, threshold at x= ω_2

$$I^2_{(\omega_2)} = \frac{I^2_{0,2}}{{\omega_2}^2 2\pi} e^{-2} \tag{10}$$

When threshold becomes equal,

$$\frac{I^2_{0,1}}{{\omega_1}^2 2\pi} e^{-2} = \frac{I^2_{0,2}}{{\omega_2}^2 2\pi} e^{-2} \tag{11}$$

This can be simplified so that

$$\frac{\omega_2^2}{\omega_1^2} = \frac{I^2_{0,2}}{I^2_{0,1}} e^{-2}, \alpha = \frac{\omega_2^2}{\omega_1^2} = \sqrt{\frac{I_{0.2}}{I_{0,1}}} \tag{12}$$

Thus,

$$\frac{A}{V} = \frac{1}{\sqrt{\frac{I_{0.2}}{I_{0,1}}}} \tag{13}$$

which means that the ratio of surface area to volume ratio is inversely related to the normalized excitation power, which is related to the diffusion time. This inverse relationship is demonstrated in the data (Figure 9) and explains why shorter diffusion times are obtained at higher excitation intensities.

S2—Supplementary data

Figure S1 Effect of time binning using 40× objective lens

The impact of time binning on autocorrelation function and diffusion time obtained from Rhodamine B solution at 10 nM concentration is demonstrated in Figure S1. As shown in the figure, the FCS data obtained from 40× (NA 0.8) is plotted for different time binning which is varied from 10^3 ns to 10^7 ns. Similar to the 63× objective, it is visible from the figure that autocorrelation of the photon arrival time is not evident at shorter time binning (1000 ns) and longer time binning (10^7 ns) where autocorrelation function is hardly recognizable.

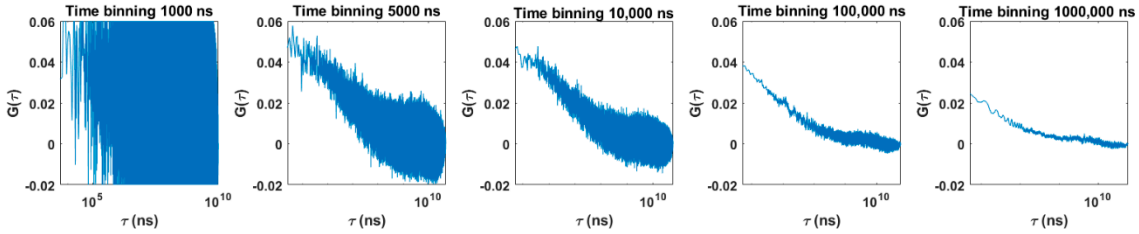

Figure S1. The effect of time binning on generating FCS curve obtained from Rhodamine B solution at a concentration of 10 nM. The data was obtained from red channel (580/150 nm) at 800 nm excitation wavelength, 25 mW excitation intensity using 40× (NA 0.8) objective lens.

Figure S2—Effect of time binning on photon count using 40× objective lens

Figure S2 demonstrates the consequences of time binning of the photon arrival time on average photon count rate obtained from Rhodamine B solution (10 nM) excited at 800 nm at 25 mW. The average photon count rate increases as time binning increases, similar to the results observed for 63× objective. It is evident from the figure that the photon count becomes stable over the time range as time binning approach 10^4 ns.

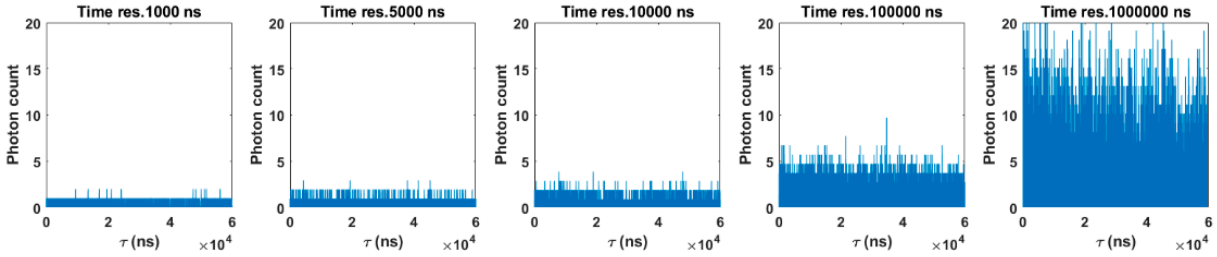

Figure S2. The effect of time binning on photon count rate obtained from Rhodamine B solution at concentration 10 nM. The data was obtained from red channel (580/150 nm) at 800 nm excitation wavelength, 25 mW excitation intensity using 40× (NA 0.8) objective lens.

Figure S3—Autocorrelation parameters as a function of excitation power

Figure S3 shows the excitation intensity as a function of amplitude of the autocorrelation function (G(0)) and average photon count obtained from fluorescence correlation data generated from Rhodamine B solution (10 nM) using 40× (NA 0.8) objective lens. As similar to 63× objective, the amplitude of the autocorrelation function decays with increasing excitation intensity and it is shown in the figure. The number of particles (N) is extracted from G(0) as N and G(0) has an inverse relationship. At a constant concentration, N becomes proportional to the excitation volume. Therefore, data (N) is fitted to a curve ($N \sim (I/I_0)^{3/2}$) and thus Go is fitted to the curve defined by the relationship $G(0) \sim 1/(I/I_0)^{3/2}$) as shown in Figure S4a,b. As expected, average photon count obtained from 40× objective lens follows a quadratic behaviour (slope ~2) as normal two photon excitation [3]. Furthermore, there is no evidence for photobleaching or excitation saturation in contrast to the previous reports [4–6].

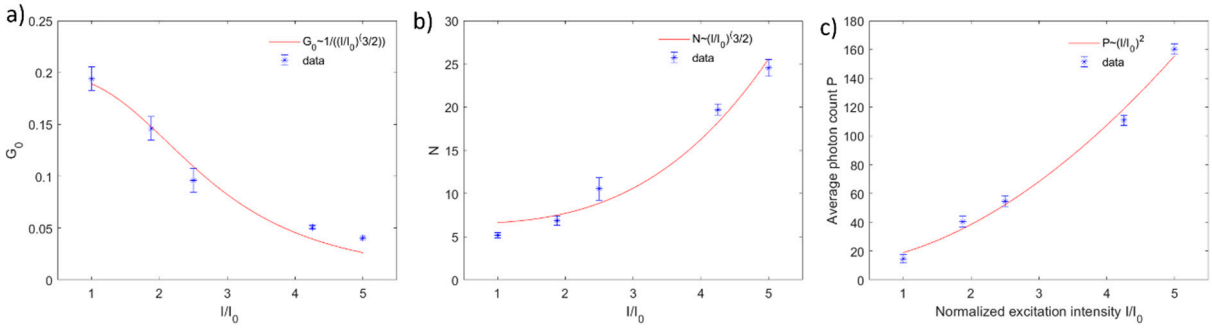

Figure S3. Plot of the a) autocorrelation amplitude function G(0) acquired using simple data fit ($G_0 \sim (I/I_0)^{3/2}$) and b) number of particles N using data fit ($N \sim (I/I_0)^{3/2}$) on autocorrelated data (time binning 10,000 ns) from experimental measurements of a Rhodamine B solution (10 nM), the 40× (NA 0.8) objective lens as a function of different laser powers, c) average photon count as a function of excitation power. Data points in blue and red line is fitting.

Figure S4–Diffusion time as a function of excitation intensity

Figure S4 shows the relationship between diffusion time and excitation intensity for 40× objective lens. The behaviour is similar to the results obtained from 63× objective lens. The diffusion time becomes faster at higher excitation intensities and slower at lower excitation levels as shown in the figure. This confirms that the proposed hypothesis follows for both objectives. Further study is required.

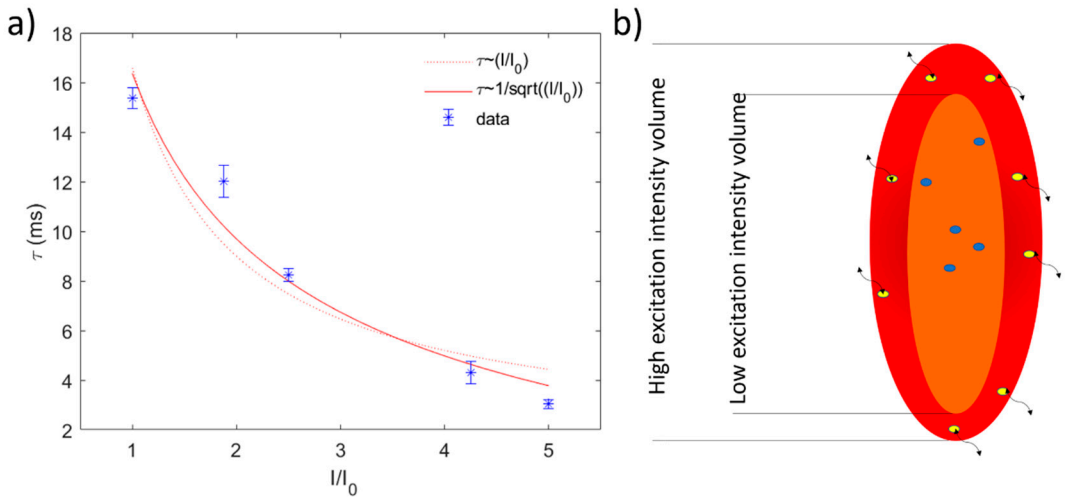

Figure S4. a) Plot of the diffusion time acquired using simple data fit ($\tau \sim 1/(I/I_0)^{0.5}$on autocorrelated data 10,000 ns) from experimental measurements of a Rhodamine B solution (10 nM), the 40× (NA 0.8) objective lens as a function of different laser powers. Data points in blue. Red lines represents fitting to two different models ($\tau \sim 1/(I/I_0)^{0.5}$ and $\tau \sim (I/I_0)$) demonstrating a 1/r dependency where r is related to the size of focal volume, which will increase as laser power increases (b).

S3—MATLAB code

The time tagged photon arrival data were time binned using different binning settings, and the time-binned data were subject to autocorrelation by utilising a customised algorithm, inspired by others [7], implemented in MATLAB (MathWorks Inc.).

The full MATLAB code will be available by contacting the corresponding authors.

References

1. Denk, W.; Strickler, J. H.; Webb, W. W. Two photon laser scanning fluorescence microscopy, *Science (New York, N.Y.)* **1990,** 248, (4951), 73–6.
2. Lakowicz, J. R., Principles of fluorescence spectroscopy. 2006; p 1–954.

3. Zipfel, W. R.; Williams, R. M.; Webb, W. W. Non-linear magic: multiphoton microscopy in life scinces, *Nature Biotechnology* **2003,** 21, (11), 1369-1377.
4. Berland, K.; Shen, G. Excitation saturation in two-photon fluorescence correlation spectroscopy, *Applied optics* **2003,** 42, (27), 5566-–5576.
5. Petrášek, Z.; Schwille, P. Photobleaching in Two-Photon Scanning Fluorescence Correlation Spectroscopy, *ChemPhysChem* **2008,** 9, (1), 147–158.
6. Hess, S. T.; Webb, W. W., Focal Volume Optics and Experimental Artifacts in Confocal Fluorescence Correlation Spectroscopy *Biophys J* **2002,** 83, (4), 2300–2317.
7. Laurence, T. A.; Fore, S.; Huser, T. , Fast, flexible algorithm for calculating photon correlations*Opt Lett* **2006,** 31, (6), 829–31.